https://doi.org/10.20965/jdr.2018.p1257

Survey Report:

Dynamic Integrated Model for Disaster Management and Socioeconomic Analysis (DIM2SEA)

Erick Mas[*1,†], Daniel Felsenstein[*2], Luis Moya[*1], A. Yair Grinberger[*2,*3], Rubel Das[*4], and Shunichi Koshimura[*1]

[*1]Laboratory of Remote Sensing and Geoinformatics for Disaster Management
International Research Institute of Disaster Science (IRIDeS), Tohoku University
468-1 Aoba, Aramaki, Aoba-ku, Sendai, Miyagi 980-8572, Japan
[†]Corresponding author, E-mail: mas@irides.tohoku.ac.jp
[*2]Department of Geography, The Hebrew University of Jerusalem, Jerusalem, Israel
[*3]GIScience Research Group, Institute of Geography, Heidelberg University, Heidelberg, Germany
[*4]Research & Development Center, Nippon Koei Co., Ltd., Tokyo, Japan
[Received August 15, 2018; accepted October 29, 2018]

The DIM2SEA research project aims to increase urban resilience to large-scale disasters. We are engaged in developing a prototype Dynamic Integrated Model for Disaster Management and Socioeconomic Analysis (DIM2SEA) that will give disaster officials, stakeholders, urban engineers and planners an analytic tool for mitigating some of the worst excesses of catastrophic events. This is achieved by harnessing state-of-the-art developments in damage assessment, spatial simulation modeling, and Geographic Information System (GIS). At the heart of DIM2SEA is an agent-based model combined with post-disaster damage assessment and socioeconomic impact models. The large amounts of simulated spatial and temporal data generated by the agent-based models are fused with the socioeconomic profiles of the target population to generate a multidimensional database of inherently "synthetic" big data. Progress in the following areas is reported here: (1) Synthetic population generation from census tract data into agent profiling and spatial allocation, (2) developing scenarios of building damage due to earthquakes and tsunamis, (3) building debris scattering estimation and road network disruption, (4) logistics regarding post-disaster relief distribution, (5) the labor market in post-disaster urban dynamics, and (6) household insurance behavior as a reflection of urban resilience.

Keywords: urban simulation, damage assessment, socioeconomic impact, disaster management, disaster simulation

1. Background

The present report reviews an integrated model developed as part of collaborative research between Japan and Israel. The final goal of this project is to generate a prototype of a Dynamic Integrated Model for Disaster Management and Socioeconomic Analysis (DIM2SEA). We are developing this model to provide tools for evaluating multiple disaster scenarios considering the impact of physical and socioeconomic effects on urban resilience. In this report, the path taken to accomplish this goal is presented.

Disasters can be large and complex incidents that are inherently challenging to manage [1], causing physical destruction to the built environment (direct losses). Consequently, this disrupts the economic activity, production, and consumption of businesses and people (indirect losses). Estimating the possible impacts of future or current disaster events is one of the main tasks of disaster prevention practitioners. To accomplish this, these practitioners require tools to effectively comprehend post-disaster conditions. However, among the numerous tools available to conduct such estimations or evaluations, most have focused on assessing individually either physical damage or economic losses [2–4]. In recent years, there has been an interest in fusing damage and loss models from a multidisciplinary perspective [5].

In addition, a disaster event provides evidence of the vulnerabilities of a community, society, or built-up area. Furthermore, society evolves (*lives*) in time because of dynamics in its socioeconomics, reaching a relative equilibrium that emerges from the interaction of various actors and their activities. Therefore, when a disaster strikes a society, it has a destructive effect not only on buildings and infrastructure, but also on people and their economic activities. It is necessary to quantify and grasp these effects as quickly as possible to understand the situation, needs and alternatives available to respond and cope with the impact. Thus, methods to rapidly quantify such physical damage are important in the disaster response stage. On the other hand, societies consist of humans who often organize themselves around economic activities such as working or commuting. Such organizations and relationships with the labor market become a sort of *respiratory system* for the economy of a society *living* in the urban

environment. Consequently, when a disaster triggers a shock, a decline in work productivity is observed, after which the system no longer *breathes* normally.

The equilibrium of physical components and socioeconomic activities contributes to growth and development; however, a lack of urban resilience can compromise a community's growth rates and aspirations. Urban resilience is a timely issue. The ravages of the Indian Ocean Tsunami (2004), Hurricane Katrina in New Orleans (2005), Haiti and Christchurch earthquakes in 2010 and 2011, 2010 Maule earthquake in Chile, Tokohu earthquake and tsunami (2011) and Superstorm Sandy (2012) among others have brought home the urban impacts of natural disasters and differential abilities of cities to mitigate them. The Sendai Framework for Disaster Risk Reduction 2015–2030 (SFDRR) adopted at the recent Third World Conference on Disaster Risk Reduction in March 2015 notes that *"it is urgent and critical to anticipate, plan for, and reduce disaster risk to effectively protect people and socioeconomic assets, amongst others, to strengthen community resilience."* The notion of resilience is prioritized in the SFDRR. However, as with many metaphors, its precise meaning is ambiguous and not seamlessly transferable to the urban context. The concept of "resilience" is rooted in the biological and ecological sciences [6, 7], and therefore, is often discussed in the context of particular physical shocks, such as ecological degradation, climatic change and natural disasters. Although the role of shocks in ecosystems may be conceptually analogous to those on cities, such comparisons are inevitably limited. The urban system responds to a set of forces very different from those that fashion the natural environment.

In the DIM2SEA Project, we aim to address two dimensions, namely, physical and socioeconomic impacts. The project focuses on enhancing disaster response and socioeconomic resilience. Specifically, we are interested in the differential socioeconomic impacts of disasters on subsectors of the population and long-term system-wide effects on the urban environment, an issue that has received scant attention in the past. In this respect, DIM2SEA fills an important gap in both technology development and disaster management practice. The modeling platform developed in the project combines short-term damage and casualty assessment, evacuation routing, and transportation disruption, along with the longer-term assessment of urban dynamics post-disaster. While the former focuses on damage, evacuation, and casualty estimation, the latter includes a simulation of longer-term structural urban changes including land use, fixed capital stock, and labor market change. These recursively impact the urban social and demographic composition, thereby mediating urban resilience. Combining these assessments and the synergic consideration of the effects and relationships between them can provide significant insights into the complexity of disasters and urban resilience.

2. Purpose and Overview

In the project, we aim to develop a prototype of DIM2SEA that will provide disaster officials, stakeholders, urban engineers, and planners with an analytic tool for mitigating catastrophic events. **Fig. 1** summarizes the components and their relationships needed to produce a comprehensive disaster management tool.

The DIM2SEA Project acts as a "what-if" scenario analysis tool filling the gap between technology development and disaster management practice. In addition, it provides a quantitative measure for urban resiliency through simulation. Scholars have proposed several dimensions by which to measure resilience [8–10]. However, these dimensions provide indexes that characterize the vulnerability of the urban environment and community preparation at a point in time (pre-disaster). In contrast, in the DIM2SEA Project, we propose a temporal measure of resilience. Through a simulation, disaster damage impacts the socioeconomic equilibrium, and the time necessary to achieve new equilibrium in the system is considered a measure of resiliency. Furthermore, by comparing multiple damage and response scenarios, the effects on urban resilience can be measured and evaluated.

First, the spatial database from the population and socioeconomic census is disaggregated at the individual level (see Section 3.1). The disaggregated population is spatially allocated in the building inventory following an iterative fitting method. Next, individuals are grouped into households to keep the generated synthetic data as similar as possible to the real census data. When earthquake and tsunami events occur, the strong ground motion is obtained from various possible sources (e.g., data recorded by seismic stations, earthquake simulation results), while tsunami inundation estimations are gathered from simulation outputs (see Section 3.2). When the situation merits it (i.e., when warnings are issued, strong ground motion is severely felt or when an individual's risk perception is high), citizens trigger their evacuation. We model evacuation behavior with the outcome of building and road disruption estimations to obtain human loss estimations and clarify the urban post-disaster situation (see Section 3.2). Once the shake or inundation has stopped, the remaining agents are expected to be in shelters or safe areas. The spatial location and amount of population at each shelter will determine the level of demand for disaster relief. Moreover, if roads have been disrupted, then an optimum logistic strategy to satisfy these demands is needed. Here, we use multiobjective optimization modeling to assess the number and locations of warehouses and tents needed for effective disaster relief (see Section 3.3). This hazard impact situation is employed as the initial condition for the post-disaster relief simulation and land-use and population dynamic estimation.

For the disaster relief simulation, after the evacuation is completed, survivors's whereabouts are known and shelter needs are assumed corresponding to the number of evacuees obtained in the simulation. The best alternatives

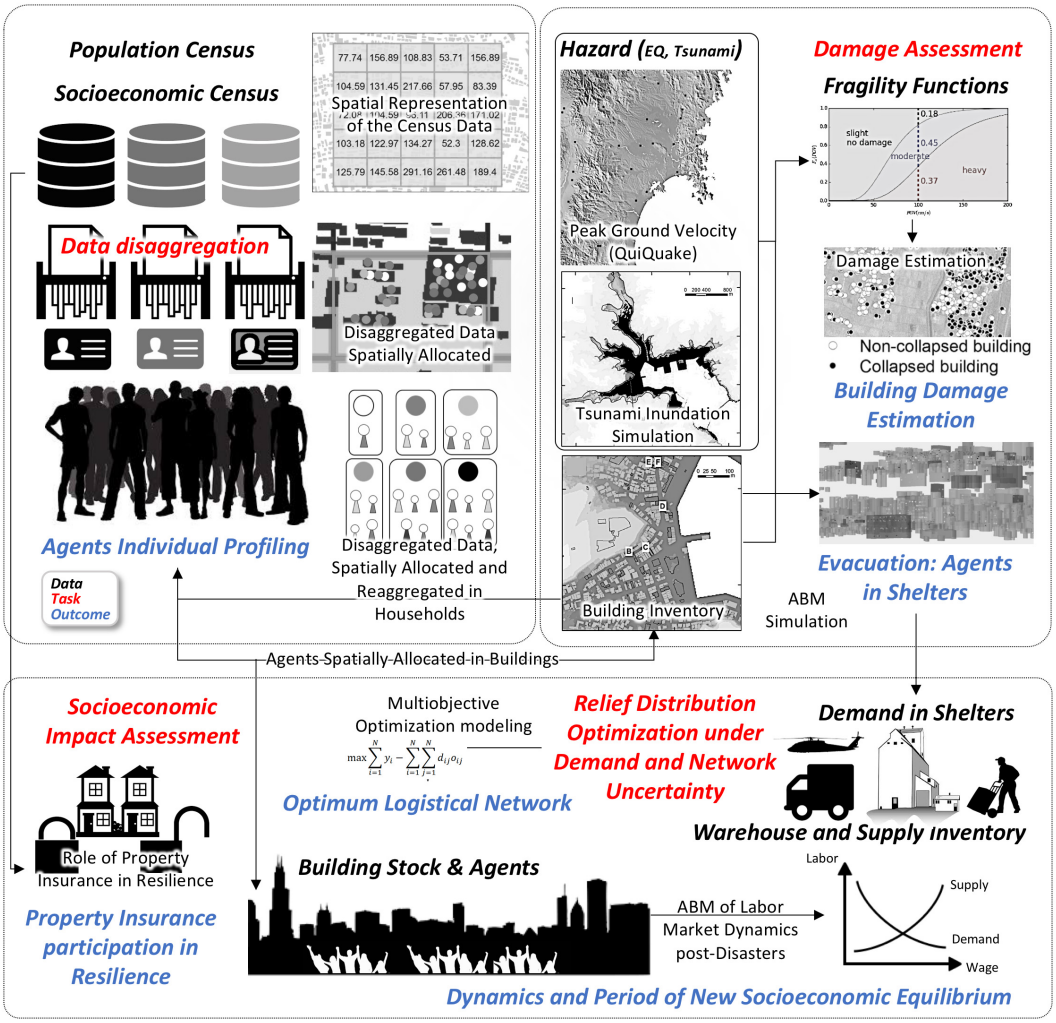

Fig. 1. Summary of tasks and outcomes conducted as part of the DIM2SEA Project.

for disaster relief response under such conditions are calculated with a time frame for evacuee attendance and migration. The dynamics of evacuees and the population in general are decided based on socioeconomic factors and the extent of the damage in the area. Thus, urban conditions and the socioeconomic profiles of households are combined into an agent-based model that produces synthetic big data and an overall view of dynamics in the simulated area. The time taken for the model's dynamics to reach equilibrium is the unit scale used to measure urban resilience. The faster an urban space adapts, the higher the resilience will be. As mentioned, the physical damage estimation is incorporated within the components of DIM2SEA; thus, building stock and property damage can be quantified. Moreover, physical destruction can also indirectly affect the labor market, which is represented here by wage levels, workforce participation, and job occupancy [11] (see Section 3.4).

3. Components of the DIM2SEA System

A data disaggregation algorithm was developed to build individual socioeconomic profiles from census tract data. The allocation of the census data into households and discrete individuals enables a deep analysis of urban and socioeconomic dynamics. The Israeli group developed a dedicated algorithm for data disaggregation and the generation of synthetic spatial microdata [4]. The approach calls on combining census tract-level data with GIS building layers to generate synthetic spatial microdata. The resultant synthetic database is detailed and accurate and represents the spatial distribution of buildings, dwelling units, households and inhabitants in the urban area.

Hazards are simulated based on their generation, propagation, and impact on the urban environment using physical and geospatial models to estimate the damage to buildings. For instance, the QuiQuake[1] system provides strong ground motion maps of peak ground velocities soon after an event. Such information comprises a valuable database of earthquake scenarios that can be combined with seis-

1. https://gbank.gsj.jp/QuiQuake/index.en.html

mic fragility curves developed elsewhere [12] to estimate the level of damage to buildings in the area. Similarly, tsunami numerical simulations combined with tsunami fragility curves [13] are also used to estimate the level of damage due to tsunamis. In addition, agent-based models are employed to estimate human losses. A model to estimate casualties during a tsunami [14] is used to test human behavior in the case of an evacuation and combine the tsunami inundation output to observe the process of evacuation in a realistic and dynamic fashion. The next component addresses the issue of a relief allocation strategy. As is well known, after a disaster, there is limited information about the areas affected and a high need for relief supplies. An optimal strategy aims to respond quickly and use relief items with a minimum amount of wastage and shortage time. An agent-based model was developed [15] to address this challenge and integrated into the DIM2SEA model. Finally, land-use and population dynamics are modeled following agent decisions based on damage conditions and socioeconomic traits. For instance, households with larger incomes and less damage to their property or workplaces may recover faster than families with a lower income and severe damage to their property [16]. The processes of decisions regarding migration and adaptation will be discussed in the future in the project and reported later. The outcome of the simulation scenarios will provide a large amount of data for multiple levels of the urban environment. This information is considered synthetic big data that must be processed for scenario analysis. The information expected at this stage is individual agents' position tracks and disaster response schedules, household composition, individual economic recovery and overall dynamic equilibrium. The methods to process this information are still under study and will be reported in the future. The geospatial information and analysis of the synthetic big data produced during the scenario modeling are presented through a web-based environment that facilitates accessibility, management and understandability. A limited interactive environment is constructed to share the scenarios and outcomes of the impact, recovery and adaptation of target areas.

3.1. Data Disaggregation and Agent Profiling

The first component in the DIM2SEA aims to generate synthetic data at a microscale level from the population census tract and socioeconomic census. In general, the urban population is represented in aggregated quantities in the area of residence. The spatial level of accuracy and resolution of this information varies between countries. This section summarizes the procedure followed to generate the synthetic population from a grid-based format of aggregated data provided by the Statistics Bureau of Japan based on the Census of 2010 in Sendai City, hereafter the Census (**Fig. 2**). The main target at this stage is to build a set of agents, where each agent will represent a citizen. Each agent must reflect certain features in the aggregated data such as age, gender, and economic profile. Furthermore, subsets of agents representing households should

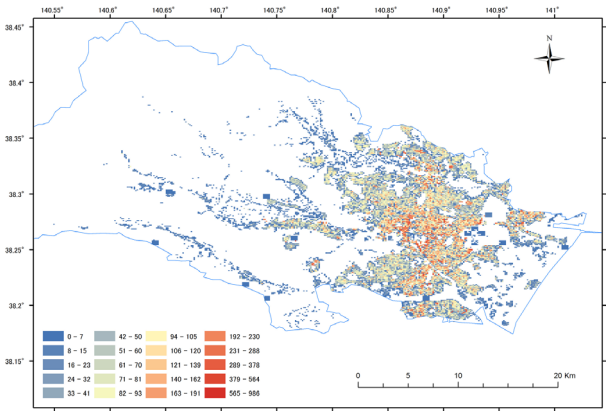

Fig. 2. Population of Sendai city, Japan.

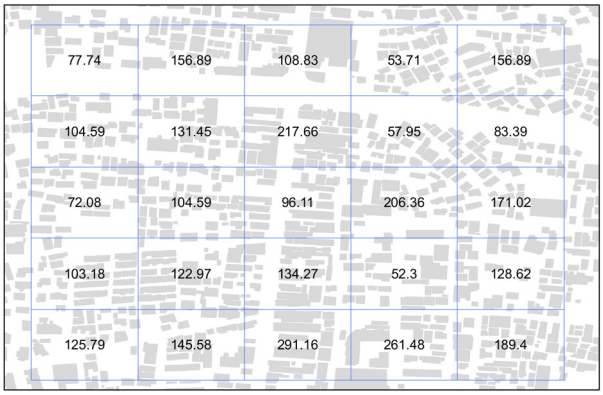

Fig. 3. Example of a fourth-order mesh composed of 25 first-order meshes. The number shown in each cell denotes an estimate of the number of citizens living inside.

be defined. Thus, the group of agents must be consistent with the aggregated values provided by the Census, also in terms of population counts and households.

Figure 2 shows the aggregate population within a uniform mesh format. Each mesh is defined by two codes: first- and fourth-order mesh codes. **Fig. 3** shows an example of a fourth-order mesh, whose dimensions are 548 m in the horizontal direction and 460 m in the vertical direction. Each fourth-order mesh is subdivided into 25 first-order meshes. **Fig. 3** also shows the number of citizens in each first-order mesh provided by the Census. It has been noted that only the total number of people in a fourth-order mesh is an integer value. Thus, it was decided to use the aggregated value of the fourth-order meshes as ancillary data. Besides the number of citizens, the Statistics Bureau of Japan provides detailed information about the population. For instance, **Table 1** depicts the population according to the range of age and gender, and **Table 2** shows the number of households defined by the number of its members. These detailed aggregated values simplify the challenge of creating highly accurate agents consistent with real information. To illustrate, the procedure to create agents with a certain age, gender and the household

Table 1. Population by gender and by age in the fourth-order mesh shown in **Fig. 3**.

Range	Total	Male	Female	Range	Total	Male	Female
0–4	111	48	63	45–49	175	83	92
5–9	114	53	61	50–54	161	76	85
10–14	104	52	52	55–59	191	80	111
15–19	179	76	103	60–64	191	92	99
20–24	301	115	186	65–69	179	79	100
25–29	320	143	177	70–74	126	64	62
30–34	313	141	172	75–79	117	43	74
35–39	263	134	129	80–84	87	33	54
40-44	233	113	120	85–	94	28	66

Table 2. Number of households of different sizes in the fourth-order mesh shown in **Fig. 3**.

Household size	Number
1 person	1102
2 people	388
3 people	239
4 people	122
5 people	36
6 people	9
>6 people	4

to which they belong is reported in detail here. Moreover, the procedure can be easily extended to allocate more attributes provided they come from the same resolution.

The problem faced here was clearly defined and solved in 1940 [17]. The census data are arranged as a two-dimensional problem and highlighted in **Table 3**. Two abstract indexes were defined to be assigned to each agent. The row index, from 0 to 35, defines whether the agent is male or female with an age within a certain range. The column index, from 0 to 6, defines the type of household to which the agent belongs. The type of household is defined based on the number of its members (see **Table 2**). Therefore, the sample universe can be represented by a matrix N of size 36×7, where for example, the element $N_{1,1}$ denotes the number of female agents whose ages are between 0 and 4 years old (see **Table 3**). The information from the Census provides only the total marginals for both the row index $r_i = \sum_j N_{i,j}$ and the column index $c_j = \sum_i N_{i,j}$; however, the elements of N are unknown and must be estimated. With this purpose in mind, the following procedure is performed. First, the total number of agents is created with age, gender and type of household assigned randomly with a uniform distribution. Then, the matrix N is constructed and subsequently adjusted for consistency with the total marginals r_i and c_j. The elements of N are adjusted using the following recursive process:

$$N_{i,j}^{k+1} = \begin{cases} N_{i,j}^{k} \dfrac{r_i}{\sum_m N_{i,m}^{k}}, & \text{if } k \text{ even} \\ N_{i,j}^{k} \dfrac{c_j}{\sum_m N_{m,j}^{k}}, & \text{if } k \text{ odd} \end{cases} \quad \ldots . \quad (1)$$

The iterations are computed until convergence is observed. **Fig. 4** shows the total marginals before and after the adjustment. Once the matrix N is adjusted, updating the agent information and rearranging the households is straightforward. Finally, the agents are geolocated to buildings. A simple criterion was selected to allocate agents to buildings. The number of households in a building is proportional to the building volume. **Fig. 5** illustrates the agents according to their age, gender, and type of household to which they belong. This process was applied to every fourth-order mesh located in Sendai city, Japan. A similar approach in the target area in Israel is described in [4].

3.2. Short-Term Damage Assessment

A series of sub-models and methodologies were developed in the Project. We call them *short-term models* because they are limited to the immediate aftermath of a hazard event. They consist of building damage estimation methodologies using hazard parameters combined with fragility functions for damage estimation. In addition, remote sensing technology was used to develop quick methods to grasp the damage in remote areas. Provided the necessary data are available, these methods are optional tools in the DIM2SEA to assess damage in the aftermath of real earthquakes or tsunamis. For the case of the DIM2SEA model, a method to generate synthetic building damage scenarios for training and scenario analysis was developed. In this section, we summarize recent developments in this area; however, the details of each can be found in the respective referenced literature.

3.2.1. Building and Road Damage

Over time, urban regions have greatly increased, and are thus at risk of earthquakes or tsunamis. In this context, building damage models are developed to estimate losses from earthquakes, tsunamis or other hazards. Traditionally, building damage estimation was performed using an intensity scale because of the lack of strong-motion instruments [18]. [19] provided one of the first estimations of earthquake loss ratios for different types of buildings, while [20] conducted a regional study of the San Francisco Bay Area and produced an estimation of losses from a major earthquake. On the other hand, [21] conducted

Table 3. Arrangement of the matrix of frequencies N and marginal totals r_i and c_j based on census data.

			HH1	HH2	HH3	HH4	HH5	HH6	HH7	
	Age	Index	0	1	2	3	4	5	6	Total (r_i)
Male	0–4	0	?	?	?	?	?	?	?	**48**
Female	0–4	1	?	?	?	?	?	?	?	**63**
Male	5–9	2	?	?	?	?	?	?	?	**53**
Female	5–9	3	?	?	?	?	?	?	?	**61**
...	...	...	...	...	...	...	...	...	...	**...**
Female	80–84	33	?	?	?	?	?	?	?	**54**
Male	85–89	34	?	?	?	?	?	?	?	**28**
Female	85–89	35	?	?	?	?	?	?	?	**66**
		Total (c_j)	**1102**	**776**	**717**	**488**	**180**	**54**	**37**	

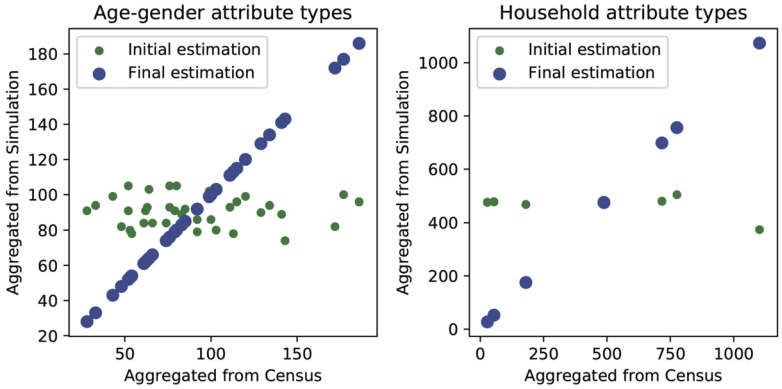

Fig. 4. Total marginals r_i (left) and c_j (right) before and after the adjustment.

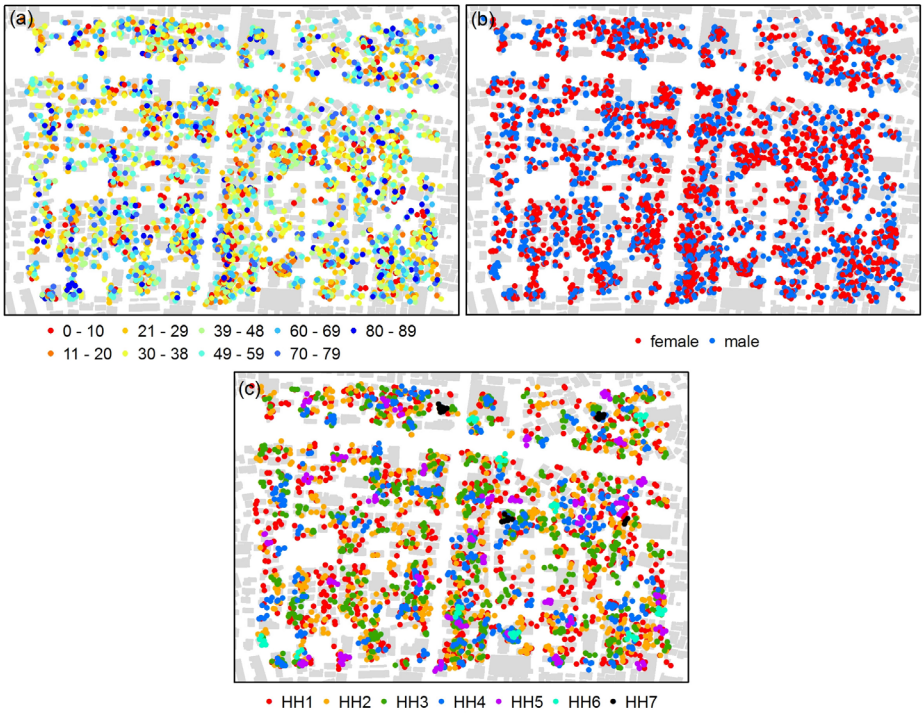

Fig. 5. Agents according to age (upper-left), gender (upper-right), and type of household (bottom).

a study following probabilistic perspectives, focusing on dwellings located in the San Francisco Bay Area in the US, which were classified into 24 classes. Considering the 12 intensities from the Modified Mercalli Intensity Scale, a 24×12 matrix was produced. Each element of the matrix contains a damage ratio and damage factor, which are the cost of repair as a percentage of replacement cost and percentage of buildings that experienced this damage ratio respectively. In addition, [22] introduced the concept of a damage probability matrix (DPM) and applied it to buildings of more than five stories. Later, the Applied Technology Council (ATC) presented detailed information about DPMs for 78 classes of structures [23]. Throughout the years, the number of studies related to earthquake loss estimation has increased considerably [24, 25], and a need for standard procedures emerged. [26] pointed out that the common methods for assessing physical vulnerability – vulnerability matrices, vulnerability curves, fragility curves and vulnerability indicators – are used in a conflicting way rather than in combination. Therefore, the HAZUS [27] method for loss estimation was developed to standardize assessments [28, 29]. On the other hand, a detailed evaluation of tsunami-induced damage considering the effects of hydrostatic forces and hydrodynamic pressures during tsunami inundation requires specific information about buildings' structural and design characteristics [30], which in most cases, is unknown. To address this issue, several authors have studied the fragility of existing buildings by constructing empirical tsunami fragility functions that present the relationship of damage probability in terms of tsunami inundation features such as flow depth and current velocity [31–34]. Tsunami fragility functions have been developed following major tsunami events such as after the 2004 Indian Ocean tsunami [13, 35, 36], 2009 Samoa Earthquake and Tsunami [37, 38], 2010 Chilean Tsunami [32], and 2011 Tohoku Tsunami [39–41]. [42] used fragility functions developed after the 2011 Tohoku Tsunami to estimate building damage and economic loss at the community level. They proposed a straightforward methodology using the maximum simulated tsunami inundation depth as an input parameter for the tsunami fragility function. This method assumes that the damage probability of a single building is characterized by the probability of damage given by the fragility function at its explanatory input variable, which in this case is the modeled inundation depth. On the other hand, [43] proposed a practical methodology to evaluate different levels of building damage using tsunami fragility functions based on two earthquake scenarios. This method considers that the damage ratio of a group of buildings within a target inundation interval is provided by the damage probability that the fragility function gives at the representative explanatory variable. In this case, the explanatory input variable is characterized by the mean value of the target inundation interval.

In our integrated model, we use the method proposed by [43] to estimate the building damage due to tsunami inundation. To estimate the damage due to an earthquake, a combination of engineering demand parameters (EDPs) such as the peak ground velocity and fragility curves is applied. A preliminary result of this assessment method was applied to damage caused by the 2016 Kumamoto earthquake [18, 44].

The estimation of damage level is based on the empirical fragility functions proposed by [12]. A fragility function provides the likelihood that an element experiences or exceeds a certain level of damage under a given EDP [45].

Fragility curves represent the relationship between a ground intensity measure (e.g., PGA, PGV, or MMI) and the likelihood that a structure experiences or exceeds a certain level of damage. Fragility curves are mostly represented as a normal or lognormal cumulative distribution function, such as:

$$\begin{aligned} F_d(x) &= P[D \geq d|X = x] \quad d\varepsilon\{1,2,\ldots,N_D\} \\ &= \Phi\left(\frac{ln(x/\theta_d)}{\beta_d}\right) \\ &\quad \ldots\ldots\ldots\ldots\ldots \end{aligned} \tag{2}$$

where $F_d(x)$ is the fragility function for damage state at d evaluated at x. $P[A|B]$ is the probability that A is true given that B is true. D is the uncertain damage state and any specific value of it is represented by d. N_D is the number of possible damage states. The ground intensity parameter is quantified by the variable X, and any specific value of it is represented by a lower case x. $\Phi(s)$ is the standard normal cumulative distribution function evaluated at β_d and θ_d, which are the median and logarithmic standard deviation respectively. The lognormal distribution is used, because it fits a variety of damage data well for either structural or nonstructural components. In addition, the lognormal distribution has zero probability density at values less than or equal to zero EDP, and it can be defined by the median and standard deviation [45]. A statistical approach is used for building the damage function, because of the source of variabilities. Ground motions with the same intensity produce a different demand on the same structure. Furthermore, buildings with the same structural system and built according to the same design code have different capacities. Thus, to use a fragility function for a given structure, a calibration of Eq. (2) is required. In other words, we need to estimate θ_d and β_d. Such estimations are based on observed data, which can be based on field surveys or analytical structural analysis. Two common methods are used to estimate parameters from the observed data: (i) the method of moments and (ii) the method of maximum likelihood. However, as clarified by [46], independent of the procedure, the parameter should be unbiased (i.e., the estimated parameters do not overestimate or underestimate the true parameter values), efficient (i.e., with small variance), and consistent (i.e., the estimated parameters converge to the true values when the number of observed data approaches infinity). A set of fragility functions for the same type of buildings with the same construction period can be used to delimit the region of each damage state. **Fig. 6** depicts the fragility curves for wooden buildings constructed during the pe-

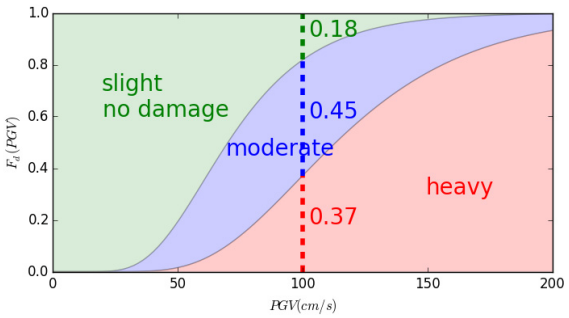

Fig. 6. Fragility functions of wood-frame (left) and reinforced concrete (right) for moderate (green line) and heavy damage (blue line).

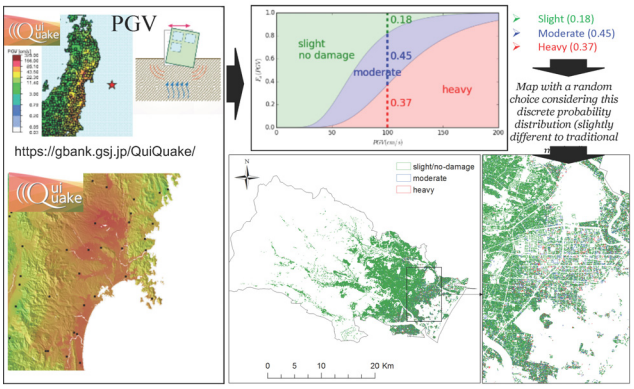

Fig. 7. Scheme of the method to estimate building damage due to an earthquake.

riod 1972–81. The set of fragility functions delimits the region of each damage state. For instance, in **Fig. 6**, a building with a demand of 100 cm/s as PGV has a probability of 0.18, 0.45, and 0.37 for slight/no damage, moderate, and heavy damage, respectively. Recall that when the demand (PGV) increases, the probability of heavy damage increases as well, while the probability of slight/no damage decreases. The probability of each damage state from the set of fragility functions is expressed as follows:

$$\begin{aligned} P[D=d|X=x] &= 1-F_1(x) && d=0 \\ &= F_d(x)-F_{d+1}(x) && 1\le d\le N \\ &= F_d(x) && d=N \\ & \quad \cdots\cdots\cdots\cdots && (3) \end{aligned}$$

It is expected that when the demand (PGV) increases, the probability of heavy damage increases, while the probability of slight/no damage decreases. The methodology applied here follows this principle and is based on an aleatory simulation in which the damage of each building is estimated from a random selection of three possible outcomes (slight/no damage, moderate, or heavy). The random selection is performed using probabilities associated with each option, which is the probability of damage calculated from the fragility curves. Furthermore, the demand parameter (PGV) is provided by the QuiQuake service,[2] which calculates the spatial distribution based on a kriging interpolation method considering an attenuation law of the strong-motion networks provided by the National Research Institute for Earth Science and Disaster Prevention (NIED).

The scheme of this approach is shown in **Fig. 7**.

To estimate the building damage due to a tsunami, we applied the method proposed by Adriano et al. [43]. Here, tsunami inundation simulations are coupled with tsunami fragility functions to observe the probable timing of building destruction and spatiality of the tsunami impact on an urban area. For details of the method and a discussion of its accuracy, see [44].

2. https://gbank.gsj.jp/QuiQuake/index.en.html

3.2.2. Human Loss and Survival Estimation

To estimate human losses and the survivability of evacuees in the case of an earthquake and tsunami we applied a simplified evacuation model tailored for large-scale urban areas. The model uses a reinforcement learning algorithm applied to the road network to calculate the best route at each node that leads to the nearest shelter or safe area. The resulting matrix of nodes and corresponding best strategy is used when simulating the movement of the population. Remember that the Census data have already been disaggregated into a micro representation of people who become agents in the agent-based model developed here. Agent-based modeling (ABM) is suitable for simulating an evacuation, because of its capability to represent evolving and changing decisions and the physical features of the environment. To estimate casualties and evacuee movement during a disaster, previous studies used agent-based models in relatively small areas [14], combining spatial urban information, evacuee preferences obtained from questionnaires and the tsunami hydrodynamic features provided by tsunami inundation modeling (for details see [47]). Within the reinforcement learning framework, the road network represents the environment in which the agents interact, and a state denotes the information an agent perceives from the environment when it is located at a certain node of the network. In a simple model, a state may be composed of the node in which the agent is located and the links available to move to another node. A more realistic model might include pedestrian density within the links, damaged links, and so on. When an agent arrives at a node, he/she has a set of options to continue moving: the links, which are called actions. The effect of every chosen action is quantified by a reward. A reward is assigned to an agent based on whether it arrived or not at an evacuation node. An agent chooses an action following a given policy. In reinforcement learning, the main target is to find the best policy that maximizes the long-term reward (i.e., the accumulated reward from the beginning to the end of the simulation), which is intimately associated with the best evacuation route.

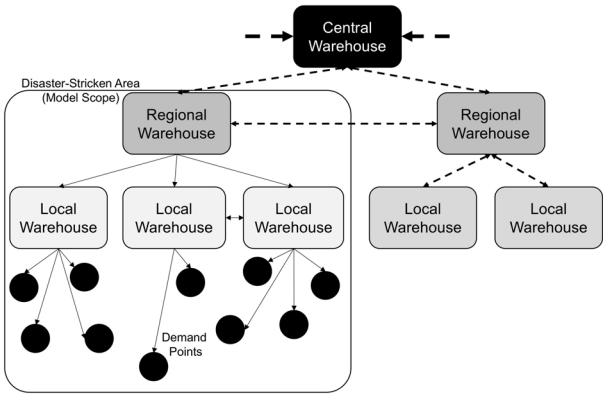

Fig. 8. Schematics of the relief support optimization model (adapted from [48]).

3.3. Disaster Relief and Logistics

The DIM2SEA model also presents two options for analysis: (i) optimization of warehouse allocation and (ii) calculation of disaster relief demand variation based on the number of evacuees in shelters. The first assessment uses a multiobjective network to maximize the area covered and minimize the distribution cost [48]. The latter calculates the day-by-day or week-by-week demand at shelters and strategy to attend and reduce the demand for the next period.

In the DIM2SEA Project, a model of the multiobjective network to select warehouse locations has been proposed [48], such that the maximum area is covered and minimum distribution cost incurred. [48] explored the relation between preparedness and response stages of the disaster management cycle. Relief demand is observed after a disaster; thus, the properties of relief demand should be studied. Therefore, the main factors of relief demand are described. The proposed model utilizes the concept of a hub-and-spoke network, because of the disruption of the transportation network and fragility of local transportation after a disaster. The spoke-hub distribution paradigm describes a series of *spokes* (i.e., routes) that connects outlying (demand) points (i.e., regional or local warehouses or shelters) to a central *hub* (i.e., central or regional warehouse) (**Fig. 8**). In addition, two performance measures for setting up a facilities network were proposed and used to determine the effectiveness of this network.

On the other hand, a model that can be used for planning disaster relief according to a desired schedule and contraction or expansion of capacities and resources is also developed. In addition, a fork of this model calculates the consecutive demand at shelters after an optimal strategy is applied based on current demand conditions. The details of this model are still being verified and will be shared by the end of the project.

3.4. Longer-Term Dynamics

Long-term models correspond to the evaluation of urban and socioeconomic dynamics in the aftermath of a disaster. For instance, work and commuting forms the daily basis of most citizens' activities. Thus, the labor market is a central feature of the urban environment and a significant shock (e.g., earthquake or other hazard) produces a market disequilibrium that contributes to delays in post-disaster recovery. The DIM2SEA project studied the labor market and modeling of its dynamics after a disaster [11] to assess long-term urban resilience from a market (re)equilibrium perspective. On the other hand, property insurance has been studied as an important ingredient of household resilience [49]. This is because much of household wealth is bound in property. Therefore, the ability to recover from property loss or damage is determined by household preferences for insurance. Looking at behavior in this market also provides the "missing link" that ties the economic and social conceptions of *resilience*. In this latter line of research, DIM2SEA uses demand for household insurance coverage as an under-recognized indicator and observed metric of revealed behavior. A simple theoretical model depicts how household preference for insurance can ultimately contribute to community resilience. Empirical evidence regarding the demand for insurance suggests that personal attributes such as age, income (wealth) and education affect household insurance behavior. In addition, physical and place-specific features such as location and topography must also be included. The expected change in wealth (loss) after the hazard determines the minimum expected level of coverage in a given location. Community resilience is defined as the sum of the marginal changes in wealth with respect to a hazard in relation to some minimum pre-defined level of resilience. The empirical strategy used in DIM2SEA to test this model considers aggregate resilience using a two-stage demand-side analysis. In the first stage, the determinants of demand for household insurance as a function of population socioeconomic attributes and characteristics of the properties covered have been estimated. As this is invariably jointly determined with personal resilience, as households with more coverage are deemed more resilient, in the second stage, the relative contribution of insurance coverage to resilience was assessed. Practicaly, this involves estimating a two-equation system consisting of an insurance share (IS) model and a personal resilience (PR) model as follows:

$$\begin{aligned} IS_i &= \alpha + \gamma PR_i + \beta X_i + \lambda Z_i + \delta D_i + \varepsilon_i \\ PR_i &= \omega + \theta IS_i + \beta X_i + \lambda Z_i + \delta D_i + \mu_i \end{aligned} \quad \ldots\ldots\ldots\ldots\ldots\ldots \quad (4)$$

where IS and PR are endogenous variables for the i-th Statistical Area (SA), X is a vector of SA-average property attributes (price, ownership, age) and Z is a vector of average SA personal characteristics (earnings inequality, share of the highly educated, and share of the elderly population), D is the distance to a hazard, ε and μ are error terms, and PR is an index. The system is estimated using ordinary least squares (OLS), two-stage least squares (2SLS), and semi-parametric least squares (SLS) estimations. To identify the insurance model, we used three

exogenous predictors of resilience that are causally unrelated to insurance: share of the Jewish population, house ownership and years of schooling. Instruments used that identify the resilience model and function as sources of exogenous variation in insurance are earnings inequality and share of the elderly population. The empirical results indicate that at the national level, instrumenting to address potential endogeneity in the relationship between insurance coverage and resilience can make a difference. At the local level, this claim is more difficult to sustain. The findings also show that personal and environmental (place-based) resilience are different sides of the same coin. In addition, the findings indicate that insurance coverage is an independent indicator of resilience different from that of classic social (personal) and economic (property or place-based) attributes. Further details about this issue can be found in [49].

However, these empirical findings are limited in terms of scope and aggregation. They only refer to spatial aggregates (i.e., statistical areas) and do not really address demand for insurance coverage. Rather, they focus on average consumer behavior, i.e., households that have chosen to purchase insurance coverage. As resilience relates to individuals and households, not statistical averages, more meaningful implementation of this component of the research program must use microdata. Currently, work is underway using microeconomic statistical modeling to understand the determinants of insurance expenditure and its relationship with the existence of natural hazards in the study area.

3.4.1. Socioeconomic Analysis: The Labor Market

A post-disaster ABM of the labor market was developed in the project [11] to simulate the economic behavior of individuals and firms. The current model (**Fig. 9**) simulates disaster outcomes relating to stock and flow attributes of the urban environment. Changes in land use (residential and nonresidential) are considered as stock attributes, while flow attributes are related to labor market conditions. Continuing with the DIM2SEA model flow, after the hazards and damage are estimated, together with population dynamics and disaster relief, capital stocks rapidly decreases and local demographics are altered, producing social changes. Specifically, the labor market is affected by a downward effect on wages. Here, we integrate with previously explained short-term models by using the damage estimation calculated at that stage. Physical damage indirectly affects the labor market.

The model described in [11] goes beyond evacuation and emergency responses. As mentioned, it moves toward a long-term view of urban recovery. Several subsystems are represented in the model, such as the labor market, housing market, and the various activities or behaviors of agents in the city.

In DIM2SEA agent-based simulations, the labor market is conceived as comprising tradable and perfectly mobile labor and a spatially rigid product market. This structure is chosen purely for agent-based simulation tractability. In this world, jobs represent the stock or labor demand side and wage levels firm reactions to local market conditions. Agents supply labor and are free to move between jobs, including those located outside the study area. Given the small size of the study area, we assume any agent seeking to commute will manage to find a job. The top-down submodel in this context deals with setting wages attached to unoccupied jobs. We introduce a parameter termed the *local clearing wage*, which is akin to the level that wage firms would offer under a closed equilibrium setting. This parameter is based on an intratemporal linear approximation of the marginal product of labor derived from a Cobb-Douglas production Eq. (5):

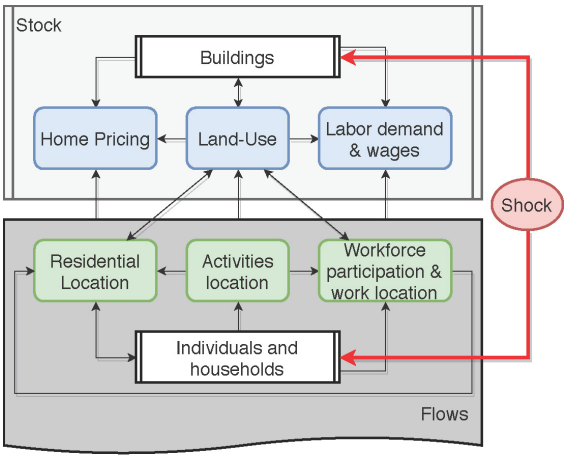

Fig. 9. Framework of the ABM of the labor market (adapted from [11]).

$$\log\left(\frac{W_t}{W_{t-1}}\right) = \alpha \log\left(\frac{K_t}{K_{t-1}}\right) + (\beta - 1)\log\left(\frac{L_t}{L_{t-1}}\right)$$

$$W_t = W_{t-1} \cdot \frac{K_t^{\alpha}}{K_t^{\alpha} \cdot \left(\frac{L_{d,t}}{L_{d,t-1}}\right)^{1-\beta}} \quad \ldots\ldots\ldots\ldots\ldots\ldots\ldots\ldots \quad (5)$$

where W_t represents clearing wage levels, K_t indicates capital stock levels, $L_{d,t}$ represents the demand for labor at time t, and β and α are Cobb Douglas parameters. The floor-space volume represents capital stock, and the share of occupied jobs represents the demand for labor from all jobs. Changes to the value of this latter parameter trickle down to the level of the individual unoccupied job (the model assumes that firms are unable to adjust the wages of occupied jobs), whose value shifts with the change in clearance wage levels. Individual agents react to these changing wage levels and their actions form the supply side. Based on these changes, agents may decide to join the workforce, and the larger the increase in the clearing wage, the higher the number of agents attracted. Unemployed agents constantly look for an open position that satisfies their requirements. We compute the attractiveness of a specific workplace as a function of the wage offered and the commuting distance required from the

agent:

$$S_{i,j} = \alpha . \frac{d(h_i, b_j)}{\max\{d(k, b_j) : k \in B\}} + (1-\alpha) . \frac{w_j - \min(w_k : \forall k \in J)}{\max(w_k : k \in J) - \min w_k : k \in J} \quad \ldots\ldots\ldots\ldots\ldots\ldots\ldots\ldots \quad (6)$$

where $S_{i,j}$ is the attractiveness score of an unoccupied job j for agent i, α is used to weight the different components, h_i is agent i's residential location, b_j is job j's location, w_j is the wage offered by job j, $d(x,y)$ is the network distance between locations x and y, B is the entire buildings set, and J is the set of unoccupied jobs.

This specific formulation is driven by the assumption that judgments are relative and agents substitute wages with commuting distance. In this case, agents are willing to accept a cut in wages if this allows them to reduce their commute. Agents' preference scores are computed according to their previous workplace characteristics or randomly if they were never employed. Agents are not assumed to have perfect information, and their capabilities are constrained to considering only seven unoccupied jobs at each iteration. When failing to find a job, an agent may decide to commute out of the area or leave the labor force. This decision is random and becomes more probable the longer the agent's job search lasts. If an agent decides to commute, its income is defined by the expected wage from the previous employment or randomly. Finding a position within the study area alters not only the agent's earnings but also those of its household.

To illustrate the simulation capabilities of the DIM2SEA agent-based model, we consider labor market outcomes of a hypothetical earthquake in the real-world environment of the Jerusalem city center. This is a mixed-land use area measuring 1.45 km^2 and housing 717 residential buildings (243,000 m^2), 179 public-use buildings (420,000 m^2), and 119 commercial structures (505,000 m^2). It also includes two major commercial locations, namely the city center and an enclosed market. We ran the model 25 times with no shock and 25 times with a simulated earthquake shock that destroys capital stock (land use change). The shock is located randomly in space (to avoid spatially biased results) and occurs at day 60. This run-in period, where land-use changes are allowed only after the first 30 days, was selected so that the system can reorganize according to the simulation dynamics before the shock. The simulations run for three years after the shock. We present aggregate results for key labor market parameters, using indicators such as changes in population over time, average wages, job occupancy rates and labor force participation and floor-space volume by use. For example, **Fig. 10** demonstrates the dynamics of the change in population, labor force participation and local employment in a scenario due to the simulated shock. As agents (workers) are mobile, they are more flexible and respond more quickly to the new situation post-disaster. In this new environment, a surplus of workers emerges consequent to falling demand and the declining attractiveness of available opportunities. However, this situation is unsustainable. Unemployed workers (agents) are forced to find other work solutions by either commuting or opting out of the workforce. This process decreases participation and local employment rates at a much faster rate than in the no-shock scenario, until stabilizing at a low-level stable equilibrium (**Fig. 10**). This result is accentuated by a population growth experienced due to an increase in the supply of housing, following a decrease in the size of the non-residential stock (**Fig. 10**). Since some migrants start as commuters, local employment rates suffer more than workforce participation and experience a much sharper decline. These dynamics portray not only land use shifts toward residential uses but also a local workforce that becomes more dominated by commuters. The city center area experiences a suburbanization trend, which reduces the total production in the region. This situation is not due to declining worker productivity, but to a change in the mixture of products offered in the area. The replacement of productive firms by residents who choose to produce in other regions amplifies this trend, reducing local productivity.

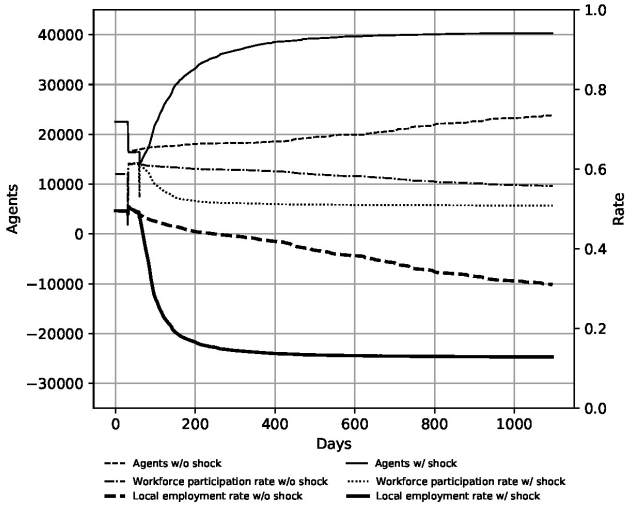

Fig. 10. Dynamics of changes in the population, labor force participation and local employment by scenario.

4. Visualization

Several models were developed in the Python or MATLAB® programming language and environments with output formats suitable for export to and representation on a GIS platform. Thus, for visualization, we combined several products of the possible spatial representation into a GIS interactive environment on a dedicated GIS server. At the time of this manuscript report, the GIS service is not public since its development is ongoing until the end of the project. However, a future link

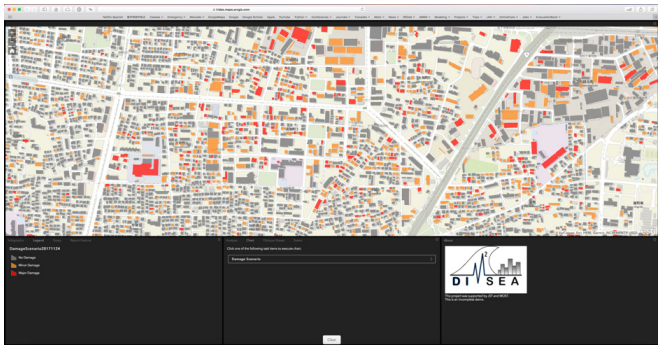

Fig. 11. Screenshot of ArcGIS Online environment for DIM2SEA model output visualization.

to this service will be posted on our project webpage.[3] An example visualization of damage scenarios is presented in **Fig. 11**.

5. Conclusions

In this development report, we presented and described the DIM2SEA model. DIM2SEA stands for Dynamic Integrated Model for Disaster Management and Socioeconomic Analysis. The purpose of this tool is to aid disaster stakeholders, responders and decision makers in experimenting with various urban disaster and recovery scenarios. We have concluded our development of the short-term damage estimation tools and population disaggregation algorithms. We are currently expanding our evacuation models for large-scale simulations. In addition, disaster relief agent-based models are in the testing stage and will soon be integrated into the whole framework of the DIM2SEA model. Finally, agent-based labor market models have been implemented, and microeconomic statistical modeling is currently underway to understand the determinants of insurance expenditure and its relationship with the existence of natural hazards in the study area. Further results for each component of the DIM2SEA can be verified in [11, 18, 44, 48–54].

Acknowledgements

This research is conducted thanks to the support of the Japan Science and Technology Agency (JST) through the SICORP project "Increasing Urban Resilience to Large Scale Disaster: The Development of a Dynamic Integrated Model for Disaster Management and Socioeconomic Analysis (DIM2SEA)." In addition, we would like to thank the International Research Institute of Disaster Science (IRIDeS) at Tohoku University. The contents of this paper were partially presented at the CUPUM2017 Conference held July 10–14, 2017, and components of the DIM2SEA model have been published elsewhere according to the referenced citations.

3. https://dim2sea.huji.ac.il

References:

[1] A. K. Donahue and R. V. Tuohy, "Lessons We Don't Learn: A Study of the Lessons of Disasters, Why We Repeat Them, and How We Can Learn Them," Homeland Security Affairs, Vol.II, No.2, pp. 1-28, 2006.

[2] T. Katada and N. Kuwasawa, "Development of tsunami comprehensive scenario simulator for risk management and disaster education," Trans. of the Japan Society of Civil Engineers (D), Vol.62, No.3, pp. 250-261, 2006.

[3] S. Koshimura, "Establishing the Advanced Disaster Reduction Management System by Fusion of Real-Time Disaster Simulation and Big Data Assimilation," J. Disaster Res., Vol.11, No.2, pp. 164-174, 2016. https://www.fujipress.jp/jdr/dr/dsstr001100020164, doi:10.20965/jdr.2016.p0164.

[4] A. Y. Grinberger and D. Felsenstein, "A Tale of Two Earthquakes: Dynamic Agent-Based Simulation of Urban Resilience," G. Lombard, E. Stern, and G. Clarke (eds.), Applied Spatial Modeling and Planning, pp. 134-154, Taylor and Francis, 2017.

[5] G. P. Cimellaro, C. Renschler, A. M. Reinhorn, and L. Arendt, "PEOPLES: A Framework for Evaluating Resilience," J. of Structural Engineering, Vol.142, No.10, pp. 04016063, 2016. http://ascelibrary.org/doi/10.1061/%28ASCE%29ST.1943-541X.0001514, doi:10.1061/(ASCE)ST.1943-541X.0001514.

[6] C. S. Holling, "Resilience and Stability of Ecological Systems," Annual Review of Ecology and Systematics, Vol.4, No.1, pp. 1-23, 1973. http://www.annualreviews.org/doi/10.1146/annurev.es.04.110173.000245, doi:10.1146/annurev.es.04.110173.000245.

[7] N. Adger, "Social Capital, Collective Action, and Adaptation to Climate Change," Economic Geography, Vol.79, No.4, pp. 387-404, 2003. http://www.jstor.org/stable/30032945, doi:10.1111/j.1944-8287.2003.tb00220.x.

[8] M. Bruneau, S. E. Chang, R. T. Eguchi, G. C. Lee, T. D. O'Rourke, A. M. Reinhorn, M. Shinozuka, K. Tierney, W. A. Wallace, and D. v. Winterfeldt, "A Framework to Quantitatively Assess and Enhance the Seismic Resilience of Communities," Earthquake Spectra, Vol.19, No.4, pp. 733-752, 2003. https://doi.org/10.1193/1.1623497, doi:10.1193/1.1623497.

[9] B. H. N. Razafindrabe, G. A. Parvin, A. Surjan, Y. Takeuchi, and R. Shaw, "Climate Disaster Resilience: Focus on Coastal Urban Cities in Asia," Asian J. of Environment and Disaster Management (AJEDM) – Focusing on Pro-active Risk Reduction in Asia, Vol.01, No.01, p. 101, 2009. http://rpsonline.com.sg/journals/101-ajedm/2009/0101/S179392402009000088.xml, doi:10.3850/S179392402009000088.

[10] R. D. Kusumastuti, Viverita, Z. A. Husodo, L. Suardi, and D. N. Danarsari, "Developing a resilience index towards natural disasters in Indonesia," Int. J. of Disaster Risk Reduction, Vol.10, No.PA, pp. 327-340, 2014. http://dx.doi.org/10.1016/j.ijdrr.2014.10.007, doi:10.1016/j.ijdrr.2014.10.007.

[11] A. Y. Grinberger and P. Samuels, "Modeling the labor market in the aftermath of a disaster: Two perspectives," Int. J. of Disaster Risk Reduction, Vol.31, pp. 419-434, 2018. https://linkinghub.elsevier.com/retrieve/pii/S2212420918306514, doi:10.1016/j.ijdrr.2018.05.021.

[12] O. Murao and F. Yamazaki, "Development of Fragility Curves for Buildings Based on Damage Survey Data of a Local Government After the 1995 Hyogoken-Nanbu Earthquake," J. of Structural Construction Engineering, AIJ, Vol.527, No.Jan, pp. 189-196, 2000.

[13] S. Koshimura, T. Oie, H. Yanagisawa, and F. Imamura, "Developing Fragility Functions for Tsunami Damage Estimation using Numerical Model and Post-Tsunami Data from Banda Aceh, Indonesia," Coastal Engineering J., Vol.51, No.3, pp. 243-273, 2009. http://www.worldscinet.com/cej/51/5103/S0578563409002004.html, doi:10.1142/S0578563409002004.

[14] E. Mas, A. Suppasri, F. Imamura, and S. Koshimura, "Agent-based Simulation of the 2011 Great East Japan Earthquake/Tsunami Evacuation: An Integrated Model of Tsunami Inundation and Evacuation," J. of Natural Disaster Science, Vol.34, No.1, pp. 41-57, 2012. http://www.jsnds.org/contents/jnds/34_1_3.pdf, doi:10.2328/jnds.34.41.

[15] R. Das and S. Hanaoka, "An agent-based model for resource allocation during relief distribution," J. of Humanitarian Logistics and Supply Chain Management, Vol.4, No.2, pp. 265-285, 2014. http://www.emeraldinsight.com/doi/abs/10.1108/JHLSCM-07-2013-0023, doi:10.1108/JHLSCM-07-2013-0023.

[16] S. Subaiya, C. Moussavi, A. Velasquez, and J. Stillman, "A rapid needs assessment of the rockaway peninsula in New York city after hurricane sandy and the relationship of socioeconomic status to recovery," American J. of Public Health, Vol.104, No.4, pp. 632-638, 2014. doi:10.2105/AJPH.2013.301668.

[17] W. E. Deming and F. F. Stephan, "On a Least Squares Adjustment of a Sampled Frequency Table When the Expected Marginal Totals are Known," The Annals of Mathematical Statistics, Vol.11, No.4, pp. 427-444, 1940. http://projecteuclid.org/euclid.aoms/1177731829, doi:10.1214/aoms/1177731829.

[18] L. Moya, E. Mas, S. Koshimura, and F. Yamazaki, "Synthetic building damage scenarios using empirical fragility functions: A case study of the 2016 Kumamoto earthquake," Int. J. of Disaster Risk Reduction, Vol.31, No.October 2017, pp. 76-84, 2018. https://doi.org/10.1016/j.ijdrr.2018.04.016, doi:10.1016/j.ijdrr.2018.04.016.

[19] J. R. Freeman, "Earthquake Damage and Earthquake Insurance: Studies of a Rational Basis for Earthquake Insurance, Also Studies of Engineering Data for Earthquake-resisting Contruction," McGraw-Hill, 1932. https://books.google.co.jp/books?id=Tnw0AAAAMAAJ.

[20] S. T. Algermissen, J. Dewey, and W. Rinehart, "A study of earthquake losses in the San Francisco Bay area; data and analysis," 1972. http://hdl.handle.net/2027/uc1.31822013112115.

[21] K. Steinbrugge, F. McClure, and A. Snow, "Studies in seismicity and earthquake damage statistics," Technical Report, prepared for the U.S. Coast and Geodetic Survey, Department of Housing and Urban Development, Washington D.C., 1969.

[22] R. V. Whitman, "Damage Probability Matrices for Prototype Buildings," Technical Report 380, National Science Foundation, 1973.

[23] ATC-13, "Earthquake Damage Evaluation Data for California," Applied Technology Council, Redwood City, 1985. https://www.atcouncil.org/pdfs/atc13.pdf [accessed XX XX, XXXX]

[24] R. Reitherman, "A Review of Earthquake Damage Estimation Methods," Earthquake Spectra, Vol.1, No.4, pp. 805-847, 1985. http://earthquakespectra.org/doi/10.1193/1.1585293, doi:10.1193/1.1585293.

[25] Federal Emergency Management Agency (FEMA), "Assessment of State-of-the-Art Earthquake Loss Estimation Methodologies (FEMA-249)," Technical Report, 1994.

[26] M. Papathoma-Köhle, "Vulnerability curves vs. vulnerability indicators: application of an indicator-based methodology for debris-flow hazards," Natural Hazards and Earth System Sciences, Vol.16, No.8, pp. 1771-1790, 2016. https://www.nat-hazards-earth-syst-sci.net/16/1771/2016/, doi:10.5194/nhess-16-1771-2016.

[27] Federal Emergency Management Agency (FEMA), "Hazus Tsunami Model Technical Guidance," Washington DC, Vol.1, No.November, 2017.

[28] C. A. Kircher, A. A. Nassar, O. Kustu, and W. T. Holmes, "Development of Building Damage Functions for Earthquake Loss Estimation," Earthquake Spectra, Vol.13, No.4, pp. 663-682, 1997. http://earthquakespectra.org/doi/10.1193/1.1585974, doi:10.1193/1.1585974.

[29] C. A. Kircher, R. V. Whitman, and W. T. Holmes, "HAZUS Earthquake Loss Estimation Methods," Natural Hazards Review, Vol.7, No.2, pp. 45-59, 2006. http://ascelibrary.org/doi/10.1061/%28ASCE%291527-6988%282006%297%3A2%2845%29, doi:10.1061/(ASCE)1527-6988(2006)7:2(45).

[30] S. Park, J. W. v. d. Lindt, D. Cox, R. Gupta, and F. Aguiniga, "Successive Earthquake – Tsunami Analysis to Develop Collapse Fragilities," J. of Earthquake Engineering, Vol.16, No.6, pp. 851-863, 2012. http://www.tandfonline.com/doi/abs/10.1080/13632469.2012.685209, doi:10.1080/13632469.2012.685209.

[31] S. Koshimura, Y. Namegaya, and H. Yanagisawa, "Tsunami Fragility – A New Measure to Identify Tsunami Damage –," J. Disaster Res., Vol.4, No.6, pp. 479-488, 2009.

[32] E. Mas, S. Koshimura, A. Suppasri, M. Matsuoka, M. Matsuyama, T. Yoshii, C. Jimenez, F. Yamazaki, and F. Imamura, "Developing Tsunami fragility curves using remote sensing and survey data of the 2010 Chilean Tsunami in Dichato," Natural Hazards and Earth System Science, Vol.12, No.8, pp. 2689-2697, 2012. http://www.nat-hazards-earth-syst-sci.net/12/2689/2012/nhess-12-2689-2012.html, doi:10.5194/nhess-12-2689-2012.

[33] A. Suppasri, S. Koshimura, M. Matsuoka, H. Gokon, and D. Kamthonkiat, "Remote Sensing: Application of remote sensing for tsunami disaster," Y. Chemin (ed.), Remote Sensing of Planet Earth, pp. 143-168, InTech, 2012.

[34] I. Charvet, J. Macabuag, and T. Rossetto, "Estimating Tsunami-Induced Building Damage through Fragility Functions: Critical Review and Research Needs," Frontiers in Built Environment, Vol.3, No.August, 2017. http://journal.frontiersin.org/article/10.3389/fbuil.2017.00036/full, doi:10.3389/fbuil.2017.00036.

[35] A. Suppasri, S. Koshimura, and F. Imamura, "Developing tsunami fragility curves based on the satellite remote sensing and the numerical modeling of the 2004 Indian Ocean tsunami in Thailand," Natural Hazards and Earth System Science, Vol.11, No.1, pp. 173-189, 2011. http://www.nat-hazards-earth-syst-sci.net/11/173/2011/, doi:10.5194/nhess-11-173-2011.

[36] N. Valencia, A. Gardi, A. Gauraz, F. Leone, and R. Guillande, "New tsunami damage functions developed in the framework of SCHEMA project: application to European-Mediterranean coasts," Natural Hazards and Earth System Science, Vol.11, No.10, pp. 2835-2846, 2011. http://www.nat-hazards-earth-syst-sci.net/11/2835/2011/, doi:10.5194/nhess-11-2835-2011.

[37] H. Gokon, S. Koshimura, M. Matsuoka, and Y. Namegaya, "Developing Tsunami Fragility Curves Due to the 2009 Tsunami Disaster in American Samoa," J. of Japan Society of Civil Engineers, Ser. B2 (Coastal Engineering), Vol.67, No.2, 2011.

[38] S. Reese, B. a. Bradley, J. Bind, G. Smart, W. Power, and J. Sturman, "Empirical building fragilities from observed damage in the 2009 South Pacific tsunami," Earth-Science Reviews, Vol.107, No.1-2, pp. 156-173, 2011. http://linkinghub.elsevier.com/retrieve/pii/S0012825211000183, doi:10.1016/j.earscirev.2011.01.009.

[39] A. Suppasri, F. Imamura, and S. Koshimura, "Tsunamigenic Ratio of the Pacific Ocean earthquakes and a proposal for a Tsunami Index," Natural Hazards and Earth System Science, Vol.12, No.1, pp. 175-185, 2012. http://www.nat-hazards-earth-syst-sci.net/12/175/2012/, doi:10.5194/nhess-12-175-2012.

[40] A. Suppasri, S. Koshimura, K. Imai, E. Mas, H. Gokon, A. Muhari, and F. Imamura, "Damage characteristic and field survey of the 2011 great east japan tsunami in miyagi prefecture," Coastal Engineering J., Vol.54, No.01, pp. 1250005, 2012. http://www.worldscientific.com/doi/10.1142/S0578563412500052, doi:10.1142/S0578563412500052.

[41] A. Suppasri, E. Mas, S. Koshimura, K. Imai, K. Harada, and F. Imamura, "Developing tsunami fragility curves from the surveyed data of the 2011 great east japan tsunami in sendai and ishinomaki plains," Coastal Engineering J., Vol.54, No.01, pp. 1250008, 2012. http://www.worldscientific.com/doi/10.1142/S0578563412500088, doi:10.1142/S0578563412500088.

[42] D. M. Wiebe and D. T. Cox, "Application of fragility curves to estimate building damage and economic loss at a community scale: a case study of Seaside, Oregon," Natural Hazards, Vol.71, No.3, pp. 2043-2061, 2013. http://link.springer.com/10.1007/s11069-013-0995-1, doi:10.1007/s11069-013-0995-1.

[43] B. Adriano, E. Mas, S. Koshimura, M. Estrada, and C. Jimenez, "Scenarios of Earthquake and Tsunami Damage Probability in Callao Region, Peru Using Tsunami Fragility Functions," J. Disaster Res., Vol.9, No.6, pp. 968-975, 2014.

[44] L. Moya, E. Mas, and S. Koshimura, "Evaluation of tsunami fragility curves for building damage level allocation," Research Report of Tsunami Engineering, Vol.34, pp. 33-41, 2017.

[45] K. Porter, R. Kennedy, and R. Bachman, "Creating fragility functions for performance-based earthquake engineering," Earthquake Spectra, Vol.23, No.2, pp. 471-489, 2007. doi:10.1193/1.2720892.

[46] J. W. Baker, "Efficient Analytical Fragility Function Fitting Using Dynamic Structural Analysis," Earthquake Spectra, Vol.31, No.1, pp. 579-599, 2015. http://earthquakespectra.org/doi/10.1193/021113EQS025M, doi:10.1193/021113EQS025M.

[47] E. Mas, S. Koshimura, F. Imamura, A. Suppasri, A. Muhari, and B. Adriano, "Recent Advances in Agent-Based Tsunami Evacuation Simulations: Case Studies in Indonesia, Thailand, Japan and Peru," Pure and Applied Geophysics, Vol.172, No.12, pp. 3409-3424, 2015. http://link.springer.com/10.1007/s00024-015-1105-y, doi:10.1007/s00024-015-1105-y.

[48] R. Das, "Disaster preparedness for better response: Logistics perspectives," Int. J. of Disaster Risk Reduction, Vol.31, No.December 2017, pp. 153-159, 2018. https://linkinghub.elsevier.com/retrieve/pii/S2212420918305806, doi:10.1016/j.ijdrr.2018.05.005.

[49] D. Felsenstein, M. Vernik, and Y. Israeli, "Household insurance expenditure as an indicator of urban resilience," Int. J. of Disaster Risk Reduction, Vol.31, No.December 2017, pp. 102-111, 2018. https://doi.org/10.1016/j.ijdrr.2018.04.008, doi:10.1016/j.ijdrr.2018.04.008.

[50] L. Moya, E. Mas, F. Yamazaki, W. Liu, and S. Koshimura, "Debris extent assessment from lidar data," New Technologies for Urban Safety of Mega Cities in Asia, p. 1, 2017.

[51] L. Moya, E. Mas, B. Adriano, S. Koshimura, and F. Yamazaki, "Building damage mapping using change detection of ALOS-2 PALSAR-2 SAR images and strong motion data," Int. Symp. on Remote Sensing, ISRS2017, pp. 281-284, 2017.

[52] L. Moya, E. Mas, B. Adriano, S. Koshimura, F. Yamazaki, and W. Liu, "An integrated method to extract collapsed buildings from satellite imagery, hazard distribution and fragility curves," Int. J. of Disaster Risk Reduction, , No.March, pp. 0-1, 2018. http://linkinghub.elsevier.com/retrieve/pii/S2212420918304047, doi:10.1016/j.ijdrr.2018.03.034.

[53] E. Mas, R. Das, L. Moya, B. Adriano, L. Urra, and S. Koshimura, "Integrated Modeling of Disaster Damage and Relief Demand Estimation in Urban Areas," Proc. of the 15th Int. Conf. on Computers in Urban Planning and Urban Management (CUPUM), pp. 1-23, 2017.

[54] L. Moya, L. Marval Perez, E. Mas, B. Adriano, S. Koshimura, and F. Yamazaki, "Novel Unsupervised Classification of Collapsed Buildings Using Satellite Imagery, Hazard Scenarios and Fragility Functions," Remote Sensing, Vol.10, No.2, pp. 296, 2018. http://www.mdpi.com/2072-4292/10/2/296, doi:10.3390/rs10020296.

Name:
Erick Mas

Affiliation:
Associate Professor, Laboratory of Remote Sensing and Geoinformatics for Disaster Management (ReGiD), International Research Institute of Disaster Science (IRIDeS), Tohoku University

Address:
468-1 Aoba, Aramaki, Aoba-ku, Sendai, Miyagi 980-8572, Japan

Brief Career:
1999-2004 B.S. Civil Eng., National University of Engineering (UNI)
2006-2009 M.Sc. in Disaster Risk Management, UNI
2009-2012 Ph.D. Civil Eng., Tsunami Eng., Tohoku University
2012-2016 Assistant Professor, ReGiD, IRIDeS, Tohoku University
2016- Associate Professor, ReGiD, IRIDeS, Tohoku University, Japan

Selected Publications:
• D. Felsenstein and E. Mas, "Introduction to SI: Modeling urban resilience to disasters," Int. J. of Disaster Risk Reduction, Vol.31, pp. 602-603, 2018.
• E. Mas, S. Koshimura, F. Imamura, A. Suppasri, A. Muhari, and B. Adriano, "Recent Advances in Agent-Based Tsunami Evacuation Simulations: Case Studies in Indonesia, Thailand, Japan and Peru," Pure and Applied Geophysics, Vol.172, Issue 12, pp. 3409-3424, 2015.
• E. Mas, A. Suppasri, F. Imamura, and S. Koshimura, "Agent Based simulation of the 2011 Great East Japan Earthquake Tsunami evacuation. An integrated model of tsunami inundation and evacuation," J. of Natural Disaster Science, Vol.34, No.1, pp. 41-57, 2012.
• E. Mas, S. Koshimura, A. Suppasri, M. Matsuoka, M. Matsuyama, T. Yoshii, C. Jimenez, F. Yamazaki, and F. Imamura, "Developing Tsunami fragility curves using remote sensing and survey data of the 2010 Chilean Tsunami in Dichato," Natural Hazards and Earth System Science, Vol.12, pp. 2689-2697, 2012.

Academic Societies & Scientific Organizations:
• Japan Society of Civil Engineers (JSCE)
• Peruvian Council of Engineers (CIP)
• American Geophysical Union (AGU)

Name:
Daniel Felsenstein

Affiliation:
Chair, Department of Geography, The Hebrew University of Jerusalem

Address:
Mount Scopus, Jerusalem 91900, Israel

Brief Career:
2002-2010 Director of the Institute of Urban and Regional Studies, Hebrew University
2004-2013 Member, National Council of Surveyors and Land Appraisers, Israel
2009-2015 Academic Director of the Center for Computational Geography, Hebrew University
2012-2016 Chair, the National Committee for Geography, Ministry of Education, Israel
2014- Consultant/National Expert to the OECD Programme on Local Economic and Employment Development (LEED)
2016- Chair, Department of Geography, The Hebrew University of Jerusalem

Selected Publications:
• D. Felsenstein, M. Vernick, and Y. Israeli, "Household Insurance Expenditure as an Indicator of Urban Resilience," Int. J. of Disaster Risk Reduction, Vol.31, pp. 102-111, 2018.
• M. Beenstock, D. Felsenstein, and D. Xieer, "Spatial Econometric Analysis of Spatial General Equilibrium," Spatial Economic Analysis, Vol.13, No.3, pp. 356-378, 2018.
• A. Y. Grinberger and D. Felsenstein, "Dynamic Agent-Based Simulation of Welfare Effects of Urban Disasters," Computers, Environment and Urban Systems, Vol.59, pp. 129-141, 2016.
• D. Felsenstein and M. Lichter, "Social and Economic Vulnerability of Coastal Communities to Sea Level Rise and Extreme Flooding," Natural Hazards, Vol.71, pp. 463-491, 2014.

Academic Societies & Scientific Organizations:
• European Regional Science Association (ERSA)
• Regional Science Association, Israeli Section
• Israeli Geographical Association
• Israeli Planners Association

Name:
Luis Moya

Affiliation:
Researcher, International Research Institute of Disaster Science (IRIDeS), Tohoku University

Address:
468-1 Aoba, Aramaki, Aoba-ku, Sendai, Miyagi 980-8572, Japan

Brief Career:
2009- Researcher, Japanese Peruvian Center for Seismic Research and Disaster Mitigation
2012-2013 Assistant Professor, National University of Engineering, Peru
2013-2015 Dr. Eng., Chiba University
2016- Researcher, International Research Institute of Disaster Science (IRIDeS), Tohoku University

Selected Publications:
• L. Moya, L. R. Marval Perez, E. Mas, B. Adriano, S. Koshimura, and F. Yamazaki, "Novel Unsupervised Classification of Collapsed Buildings Using Satellite Imagery, Hazard Scenarios and Fragility Functions," Remote Sens., Vol.10, p. 296, 2018.
• L. Moya, F. Yamazaki, W. Liu, and M. Yamada, "Detection of collapsed buildings from lidar data due to the 2016 Kumamoto earthquake in Japan," Nat. Hazards Earth Syst. Sci., Vol.18, pp. 65-78, 2018.
• L. Moya, F. Yamazaki, W. Liu, and T. Chiba, "Calculation of coseismic displacement from lidar data in the 2016 Kumamoto, Japan, earthquake," Nat. Hazards Earth Syst. Sci., Vol.17, pp. 143-156, 2017.

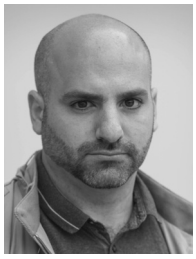

Name:
A. Yair Grinberger

Affiliation:
Post-Doctoral Researcher, Department of Geography, The Hebrew University of Jerusalem
GIScience Research Group, Institute of Geography, Heidelberg University

Address:
Room 012B Im Neuenheimer Feld 348, Heidelberg 69120, Germany

Brief Career:
2012-2017 Ph.D. Student, The Hebrew University of Jerusalem
2017-2019 Alexander von-Humboldt Fellow, The GIScience Research Group, Institute of Geography, Heidelberg University

Selected Publications:
• A. Y. Grinberger and P. Samuels, "Modeling the labor market in the aftermath of a disaster: Two perspectives," Int. J. of Disaster Risk Reduction, Vol.31, pp. 419-434, 2018.
• A. Y. Grinberger and D. Felsenstein, "Dynamic agent-based simulation of welfare effects of urban disaster," Computers Environment and Urban Systems, Vol.59, pp. 129-141, 2016.

Name:
Rubel Das

Affiliation:
Researcher, Center for Advanced Research and Development, Nippon Koei Co., Ltd.

Address:
2304 Inarihara, Tsukuba, Ibaraki 300-1259, Japan

Brief Career:
2014-2017 Assistant Professor, Tohoku University
2017- Researcher, Nippon Koei Co., Ltd.

Selected Publications:
• R. Das, "Disaster preparedness for better response: Logistics perspectives," Int. J. of Disaster Risk Reduction, Vol.31, pp. 153-159, 2018.
• R. Das and S. Hanaoka, "An Agent-Based model for resource allocation during relief distribution," J. of Humanitarian Logistics and Supply Chain Management, Vol.4, No.2, pp. 265-285, 2014.
• R. Das and S. Hanaoka, "Relief inventory modeling with stochastic lead-time and demand," European J. of Operational Research, Vol.235, No.3, pp. 616-623, 2014.

Academic Societies & Scientific Organizations:
• TRB Task Force on Humanitarian Aid Logistics, Member
• Eastern Asia Society for Transportation Studies, Member

Name:
Shunichi Koshimura

Affiliation:
Professor, International Research Institute of Disaster Science (IRIDeS), Tohoku University

Address:
468-1 Aoba, Aramaki, Aoba-ku, Sendai, Miyagi 980-8572, Japan

Brief Career:
2000-2002 Research Fellow, Japan Society for the Promotion of Science (JSPS)
2002-2005 Research Scientist, Disaster Reduction and Human Renovation Institute
2005-2012 Associate Professor, Graduate School of Engineering, Tohoku University
2012- Professor, International Research Institute of Disaster Science (IRIDeS), Tohoku University

Selected Publications:
• Y. Bai, C. Gao, S. Singh, M. Koch, B. Adriano, E. Mas, and S. Koshimura, "A Framework of Rapid Regional Tsunami Damage Recognition From Post-event TerraSAR-X Imagery Using Deep Neural Networks," IEEE Geoscience and Remote Sensing Letters, Vol.15, No.1, 2018.
• S. Koshimura, "Fusion of real-time disaster simulation and big data assimilation – Recent progress," J. Disaster Res., Vol.12 No.2, pp. 226-232, 2017.
• Y. Bai, B. Adriano, E. Mas, and S. Koshimura, "Machine learning based building damage mapping from the ALOS-2/PALSAR-2 SAR imagery: Case study of 2016 Kumamoto earthquake," J. Disaster Res., Vol.12, No.sp, pp. 646-655, 2017.

Academic Societies & Scientific Organizations:
• Japan Society of Civil Engineers (JSCE)
• Institute of Social Safety Science (ISSS)
• Japan Association for Earthquake Engineering (JAEE)
• Japan Society for Computational Engineering and Science (JSCES)
• American Geophysical Union (AGU)